Pattern Recognition of Cancer Cells Using Aptamer-Conjugated Magnetic Nanoparticles

Suwussa Bamrungsap,[†] Tao Chen,[†] Mohammed Ibrahim Shukoor,[†] Zhuo Chen,[‡] Kwame Sefah,[†] Yan Chen,[†,‡] and Weihong Tan[†,‡,*]

[†]Center for Research at Bio/nano Interface, Department of Chemistry and Department of Physiology and Functional Genomics, Shands Cancer Center, UF Genetics Institute and McKnight Brain Institute, University of Florida, Gainesville, Florida 32611-7200, United States, and [‡]State Key Laboratory of Chemo/Bio-Sensing and Chemometrics, College of Biology and College of Chemistry and Chemical Engineering, Hunan University, Changsha, 410082, People's Republic of China

ABSTRACT

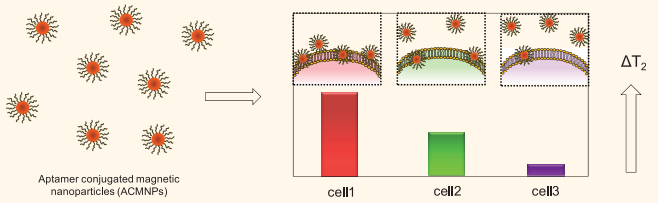

Biocompatible magnetic nanosensors based on reversible self-assembly of dispersed magnetic nanoparticles into stable nanoassemblies have been used as effective magnetic relaxation switches (MRSw) for the detection of molecular interactions. We report, for the first time, the design of MRSw based on aptamer-conjugated magnetic nanoparticles (ACMNPs). The ACMNPs capitalize on the ability of aptamers to specifically bind target cancer cells, as well as the large surface area of MNPs to accommodate multiple aptamer binding events. The ACMNPs can detect as few as 10 cancer cells in 250 μL of sample. The ACMNPs' specificity and sensitivity are also demonstrated by detection in cell mixtures and complex biological media, including fetal bovine serum, human plasma, and whole blood. Furthermore, by using an array of ACMNPs, various cell types can be differentiated through pattern recognition, thus creating a cellular molecular profile that will allow clinicians to accurately identify cancer cells at the molecular and single-cell level.

KEYWORDS: aptamer · cancer cell recognition · complex media · magnetic nanoparticle · spin–spin relaxation time

Each cancer cell line has specific intra- or extracellular biomarkers, distinguishing it from normal cells lines. Therefore, methods that can enable sensitive and selective cancer cell detection through precise molecular recognition of its biomarkers are highly desired. Recently, a novel class of ligands, known as aptamers, has been isolated and identified for such specific cancer cell recognition. Aptamers are single-stranded oligonucleotides, which recognize their targets with excellent specificity and high affinity.[1] They are generated from an *in vitro* selection process, systematic evolution of ligands by exponential enrichment (SELEX), against various targets, including ions, proteins, and even cells.[2,3] Aptamers rival antibodies for molecular recognition due to their reproducible synthesis, easy modification, good stability, and lack of immune response, making them great candidates for biosensor development and therapeutic applications.[4–6]

Many nanomaterials have been utilized for constructing biosensors based on their optical signals. However, most of them, such as quantum dots, dye-doped silica nanoparticles, or gold nanoparticles, suffer severe background interference from scattering, absorption, or autofluorescence of samples, especially in complex biological media, greatly diminishing their detection capability. In contrast, most biological samples exhibit virtually no magnetic background, and the use of magnetic nanoparticle (MNPs) can thus lead to ultrasensitive detection. Previously, we have described aptamer-conjugated nanoparticles (ACMNPs) for the collection of cancer cells, followed by detection using aptamer-conjugated fluorescent nanoparticles (ACFNPs).[7,8] This methodology provides high selectivity and sensitivity, as well as ability for multiplexed detection. However, two steps of extraction and detection were required. Although magnetic relaxation measurements have been reported for biological target detection, to the best of our knowledge, this is the first time ACMNPs have been used for sensitive cancer cell detection, as well as comprehensive cancer cell profiling. Using these ACMNPs, as few as 10 cancer cells were detected in a 250 μL sample in buffer with excellent selectivity. The sensitivity and selectivity of the system were well preserved in various complex biological media, including fetal bovine

* Address correspondence to tan@chem.ufl.edu.

Received for review January 16, 2012 and accepted March 16, 2012.

Published online March 16, 2012
10.1021/nn3002328

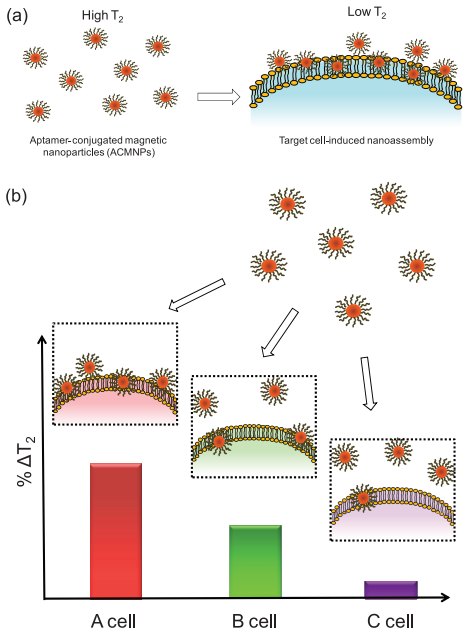

Figure 1. Schematic illustration of using the magnetic nanosensor for cancer cell detection and pattern recognition. (a) The magnetic nanoparticles conjugated with aptamers have highly specific binding to their target cells. Without target cells, ACMNPs are well dispersed, resulting in a high T_2 of surrounding water protons. The addition of target cells leads to the aggregation of magnetic nanoparticles, decreasing the T_2 of adjacent water protons. (b) Distinct recognition pattern generated for various cell lines with different receptor expression level using the magnetic nanosensor. The cell line with the most abundant (A cell) receptors gives the largest ΔT_2, followed by the cell line with the medium number of receptors (B cell), and the smallest ΔT_2 was obtained for the cell line with the lowest receptor expression level (C cell).

serum (FBS), human plasma, and whole blood. In addition, when an array of ACMNPs was used, different cell types could be discriminated through pattern recognition based on their expression level of membrane receptors. All these merits, together with the simple operation of a widely used magnetic relaxation instrument, will make ACMNP-based nanosensors useful tools for early diagnosis and effective screening of cancer.

RESULTS AND DISCUSSION

The detection mechanism of ACMNPs in solution is based on the change of spin−spin relaxation time (ΔT_2) of the surrounding water protons. When multiple ACMNPs bind to their target cells through the specific interaction between receptors on the cell membrane and aptamers on the nanoparticle surface, they act cooperatively to form clusters (Figure 1a), thereby inducing coupling of magnetic spin moment, and thus generating strong local magnetic fields.[9−11] Such strong local magnetic fields lead to inhomogeneities that accelerate the spin-dephasing of the surrounding water protons, resulting in a decreased T_2. According to the literature,[12−14] MNPs are known to enhance the magnetic resonance signal of protons from surrounding water molecules. Under these circumstances, aggregation is detected by ΔT_2, corresponding to the binding event between ligand-conjugated MNPs and target molecules. This phenomenon based on a self-amplifying proximity assay has led to the development of magnetic relaxation switches (MRSw) for the detection of small molecules, DNA/RNA, proteins/enzymes, and bacteria/viruses.[15−19]

On the basis of previous studies, some cancer biomarkers are not restricted to a certain cell line; rather, they are present in/on different cell lines or at different developmental stages of cancer.[20] For example, human protein tyrosine kinase-7 (PTK-7) is expressed on both CCRF-CEM (human leukemia) and HeLa (cervical cancer) cells.[21] Therefore, various cell lines at different physiological stages of cancer may show binding toward the same ligand, however, with different affinities, depending on their level of biomarker expression. A reliable method able to analyze various cancer cells can lead to the development of a cancer cell profile and thus a better understanding of cancer pathogenesis and the potential efficacy of new therapeutic modalities. By using an array of ACMNPs, various cell types can be differentiated through pattern recognition (Figure 1b). A cells, with the most abundant target receptors, generate the largest ΔT_2, followed by B cells, with a medium number of receptors, and then C cells, with the least number of receptors. A distinct pattern of responses generated from a set of ACMNPs would further provide a cellular profile, allowing clinicians to accurately classify and identify cancer cells at the molecular level.

The magnetic nanosensor was prepared by conjugating streptavidin-coated iron oxide nanoparticles with biotin-labeled aptamers. On the basis of the role of MNP valency on MRSw detection, which was studied by Koh and co-workers,[22] the results demonstrated that the more multivalent MNPs result in higher sensitivity of target detection. Consequently, an excess amount of biotin-labeled aptamer was used for the conjugation. The strepavidin-coated MNPs have an average hydrodynamic diameter (d) of about 30 nm and a zeta potential (ζ) of -32.4 ± 3.7 mV. Since aptamers are polyanions, the successful conjugation of aptamers on the MNPs was confirmed by the increase of negative charge on the particle's surface: a zeta potential of -41.8 ± 2.6 mV was obtained for ACMNPs. The large surface area of MNPs allows the attachment of multiple aptamers that result in simultaneous multiple interactions between ACMNPs and receptors on cell surface. The stability of the ACMNPs is excellent. No obvious aggregation and precipitation was observed even after several-month storage at 4 °C.

Although ACMNPs have been previously used for cancer cell separation,[7,8] it is still necessary to confirm that the aptamers remain viable in terms of their ability to specifically recognize their targets after conjugation.

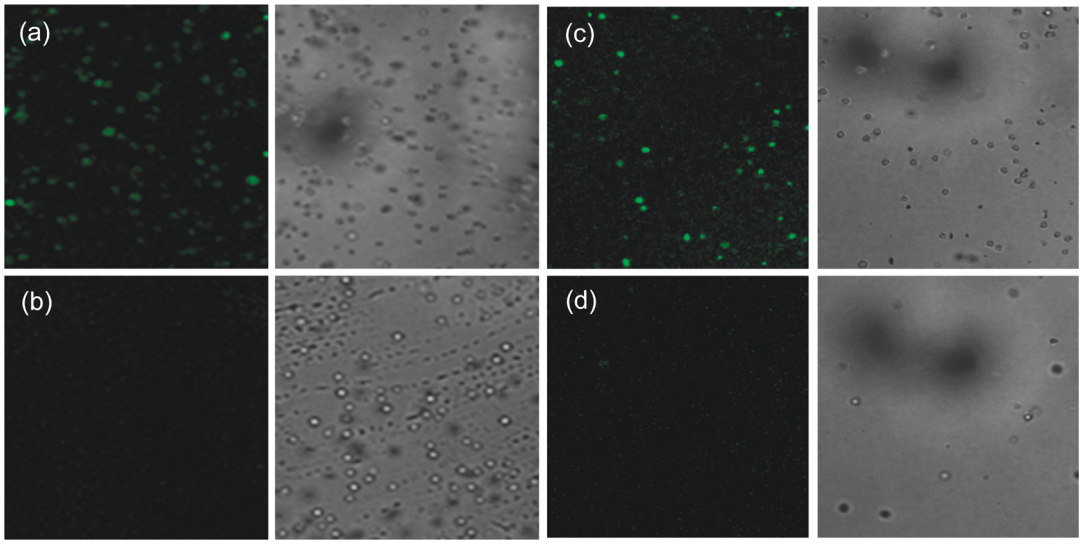

Figure 2. Specific recognition of the magnetic nanosensor to their target cancer cells. Confocal laser scanning microscope images (left: fluorescence image; right: transmission image) of CCRF-CEM cells labeled with (a) FAM-labeled sgc8c-ACMNPs (target) and (b) FAM-labeled TDO5-ACMNPs (control). Ramos cells labeled with (c) FAM-labeled TDO5-ACMNPs (target) and (d) FAM-labeled sgc8c-ACMNPs (control). Bright fluorescence signal was obtained for cells when treated with target ACMNPs, while only minimal fluorescence signal was seen for cells labeled with control ACMNPs.

Two different cell lines, CCRF-CEM cells and Ramos cells, were chosen for the demonstration. For the CCRF-CEM cells, fluorescein amidite (FAM)-labeled sgc8c-ACMNPs were used as a target and FAM-labeled TDO5-ACMNPs were used as a control. For Ramos cells, FAM-labeled TDO5-ACMNPs were used as a target and FAM-labeled sgc8c-ACMNPs were used as a control. The Sgc8c aptamer can specifically bind to PTK 7 receptors, which is highly expressed on CCRF-CEM cells, instead of Ramos cells.[23,24] TDO5 aptamer can selectively bind to IgG receptors, which is largely abundant on Ramos cells, rather than CCRF-CEM cells.[25,26] Since our aptamers were labeled with fluorescent molecule-FAM, fluorescence confocal microscopy was used to validate the target specificity of the aptamer conjugates. The binding between sgc8c-ACMNPs and CCRF-CEM cells was demonstrated by a bright fluorescence signal (Figure 2a). However, the control TDO5-ACMNPs showed only minimal fluorescence signal (Figure 2b). Similar specificity was achieved between TDO5-ACMNPs and Ramos cells: a much brighter image was obtained for the target (Figure 2c) when compared to the control (Figure 2d). These observations proved that the ACMNPs preserved the excellent biological recognition of aptamers to their targets.

After using the fluorescence technique to demonstrate the specificity of ACMNPs to their target cells, the use of the magnetic nanosensor to detect cancer cells was investigated. The first assay was performed to detect CCRF-CEM cells in phosphate buffered saline (PBS). When sgc8c-ACMNPs were mixed with CCRF-CEM cells, a decrease of T_2 was observed. To confirm that the change of T_2 was the result of specific aptamer-mediated interaction but not nonspecific aggregation of MNPs, TDO5-ACMNPs were also incubated with CCRF-CEM cells as a control, followed by the relaxation time measurements. To determine the binding, the percentage change of T_2 ($\%\Delta T_2$) was defined as follows:

$$\%\Delta T_2 = (T_{2\text{nonspiked}} - T_{2\text{sample}}) \times 100/T_{2\text{nonspiked}}$$

where $T_{2\text{sample}}$ is the average T_2 relaxation time of ACMNPs in the presence of target cells and $T_{2\text{nonspiked}}$ is the average T_2 relaxation time of ACMNPs in the absence of target cells. The results showed that 10 μg/mL was the optimal concentration for the detection of target cells (Figure 3a), since lower concentrations generated significant errors in measurement, while higher concentrations limited the detection threshold. Figure 3b showed a wide dynamic range of detection and excellent correlation between the number of target cells and $\%\Delta T_2$ using sgc8c-ACMNPs, whereas the $\%\Delta T_2$ of the control had no significant change. In addition, fewer than 10 target cells in 250 μL of PBS could be detected without any amplification method. The detection of Ramos cells was also demonstrated using their corresponding aptamer conjugates, TDO5-ACMNPs. The incubation of Ramos cells with TDO5-ACMNPs led to proportional changes of ΔT_2 with increasing number of cells, while the mixture of Ramos cells and sgc8c-ACMNPs as a control produced only small ΔT_2 changes (Supporting Information, Figure S1). These results agreed with our fluorescence assays, as described above, and confirmed the specific recognition of ACMNPs, making this a viable and practical technique for the sensitive detection of cancer cells.

The detection of mixtures of targets and nontargets (CCRF-CEM and Ramos cells, respectively) with different ratios was also demonstrated. One hundred

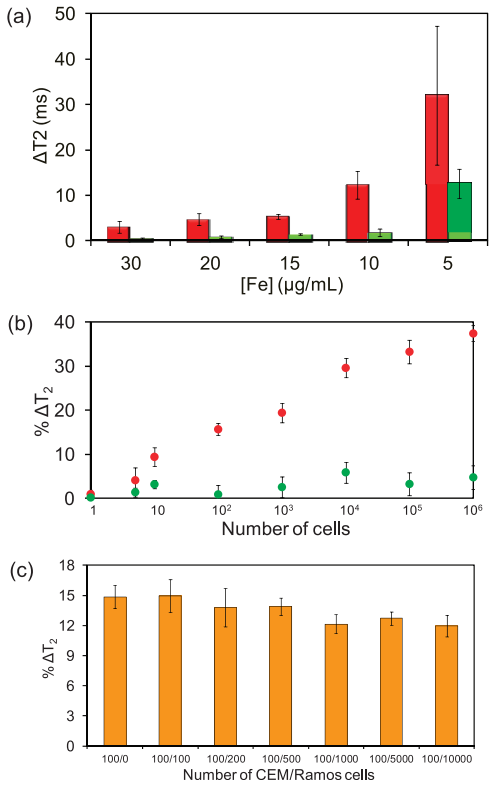

Figure 3. Use of magnetic nanosensors for target cancer cell (CCRF-CEM cell) detection in buffer systems. (a) Concentration optimization of ACMNPs in PBS (red: sgc8c-ACMNPs (target); green: TDO5-ACMNPs (control)). The higher concentrations of ACMNPs limited the detection limit, while the lower concentrations of ACMNPs generated significant error in the measurements. (b) Dynamic range determination of ACMNPs in PBS (red: sgc8c-ACMNPs (target); green: TDO5-ACMNPs (control)). A wide dynamic range was achieved, with a detection limit as low as 10 cells in a 250 μL sample volume. (c) Mimicking circulating tumor cell detection by sensing 100 target cells in a mixture of CCRF-CEM (target) and Ramos (control) cells.

CCRF-CEM cells were mixed with nontarget Ramos cells at different ratios: 1:1, 1:2, 1:5, 1:10, 1:50, and 1:100, respectively. Sgc8c-ACMNPs were used to detect the target cells, and random sequenced DNA conjugated with MNPs was used as a negative control. The results in Figure 3c showed that the target CCRF-CEM cells could be detected in mixtures of CCRF-CEM and Ramos cells with $\%\Delta T_2$ similar to those observed in the presence of target CCRF-CEM cells only. For a large number of nontarget cells, which may hinder the binding between the ACMNPs and their targets, a slight decrease of $\%\Delta T_2$ due to nonspecific interactions was observed. However, the detection in mixtures in which the ratio between target and nontarget cells was as small as 1:100 was achieved.

To further assess the potential of this technique, detection in FBS, human plasma, and whole blood samples was also performed. These assays were meant to mimic real clinical samples, which normally contain thousands of different species. The detection and quantification of CCRF-CEM cells in FBS was demonstrated

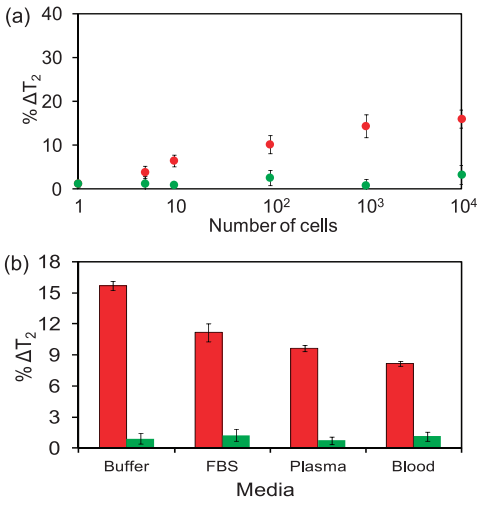

Figure 4. Use of magnetic nanosensors for target cancer cell (CCRF-CEM cell) detection in complex media (red: sgc8c-ACMNPs (target); green: TDO5-ACMNPs (control)). (a) Dynamic range determination of ACMNPs in FBS. (b) Performance comparison of ACMNPs in different complex biological media (including FBS, plasma, and blood) and PBS. All the measurements were performed using 100 target cells in a 250 μL sample volume.

by incubating CCRF-CEM-spiked FBS with sgc8c-ACMNPs. The $\%\Delta T_2$ was also proportional to the number of target cells, while the control showed only negligible changes (Figure 4a). It is important to note that this nanosensor can detect as few as 10 cells in 250 μL of FBS, which is much lower than the detection limits of conventional fluorescence- or colorimetric-based methods, which can detect in the range of thousands of cells.[27,28] Although the detection of a few target cells has been demonstrated by the chip-based diagnostic magnetic resonance system,[29] our nanosensor requires no microfabrication, and the washing step is eliminated, resulting in the simplicity and minimal detection time. Similarly, CCRF-CEM-spiked human plasma or whole blood was incubated with sgc8c-ACMNPs, followed by T_2 measurements. The results revealed that the detection and quantification of target cells can also be achieved in both human plasma and whole blood (Supporting Information, Figure S2). Nonspecific interactions in complex media containing thousands of proteins caused unwanted aggregates of ACMNPs on the cells' surfaces, producing lower relaxation times in both $T_{2\text{sample}}$ and $T_{2\text{nonspiked}}$. The low $T_{2\text{nonspiked}}$ value generated a higher background, resulting in a smaller $\%\Delta T_2$ for detection in complex media compared to detection in buffer with the same number of target cells. Nonetheless, we were able to detect as few as 100 target cells in all biological complex media (Figure 4b). This result shows promise for detection in complex biological matrixes. Successful detection of target cells in cell mixtures, FBS, human plasma, and whole blood indicates that this method can be used for cellular detection in real clinical applications.

With the successful detection of target cancer cells with high specificity and sensitivity, the use of ACMNPs to monitor the interactions between different ACMNPs and multiple cell lines was investigated. By using an array of ACMNPs combined with the use of the MRSw technique, as described above, recognition patterns were generated resulting in the differentiation of various cell types and, in turn, a cancer cell profile that could be utilized to identify and classify cancer cells more precisely than might otherwise be achieved by a single specific probe.

The target cells were chosen to represent a variety of cancer cell types: a normal lung cell line and six types of representative cancer cells, as listed in Table 1. One thousand cells of each cell line were spiked in PBS and incubated with each ACMNP individually, followed by a T_2 relaxation time measurement similar to that of the previous assays. The six cancer cell lines showed a large variation in T_2 reductions upon mixing with different ACMNPs (Figure 5). The variation of $\%\Delta T_2$ upon the incubation of multiple cell types with different ACMNPs can be explained by the different affinities of the aptamers to their target and nontarget cells. The aptamers, which have high affinity to their targets, induced ACMNPs to agglomerate on cell surface, producing large $\%\Delta T_2$, while the nontarget cells showed no significant difference in T_2. On the basis of the MR response, sgc8c-ACMNPs showed strong binding not only with their target, CCRF-CEM, but also with the DLD1 and HCT116 cell lines. It was previously described that the target of sgc8c, PTK7, is also expressed in colorectal cancers.[20] As expected, the binding of sgc8c to both colorectal cancer cell lines was observed. Similarly, KCHA10 aptamer was found to interact with most colorectal cell lines,[30] resulting in the recognition of KCHA10-ACMNPs to both HCT116 and DLD1. The other aptamers, KDED2-3, TD05, T2-KK1B10, and TSL11a, which have recognition to single cell types only, demonstrated strong specificity to their targets. Significantly, none of ACMNPs had any interaction with the normal cell line, indicating that targets of these aptamers are related only to cancer. This result also confirmed that the binding was based on the interaction of aptamer–cell surface receptors and excluded nonspecific interactions.

Furthermore, comprehensive information about the expression of specific receptors can be determined on the basis of the MR response. For example, sgc8c aptamer shows diverse $\%\Delta T_2$ on CCRF-CEM, DLD1, and HCT116 cell lines due to the different expression level of PTK7 receptor on their surface.[20,24,30] A comparative study about the expression of target receptors between malignant and host cells among three sets of data obtained from MR response, fluorescence microscope, and flow cytometry was also demonstrated by Lee and co-workers.[34] The results show that the MRSw was superior to fluorescence techniques due to shorter incubation times and higher specificity in unpurified native samples.

With the capability of our given system to quantify a small amount of target cells in various media, as described above, the pattern of recognition could also be achieved in more complicated conditions such as in biological media or with fewer cells in a similar manner. As demonstrated by El-Boubbou and co-workers, a molecular signature of different cell lines based on MR response was generated using an array of magnetic glycol nanoparticles.[35] By reducing the amount of target cells, the $\%\Delta T_2$ was decreased; however, a similar pattern of MR response was still achieved from each

TABLE 1. Representative Cell Lines and Binding Affinities of Their Selected Aptamers

cell lines	type of cell	aptamer	K_d (nM)
CCRF-CEM	leukemia	sgc8c[23] [a]	0.8
Ramos	leukemia	TDO5[25]	75.0
K562	leukemia	T2-KK1B10[31] [b]	30.0
DLD1	colon	KDED2a-3[32]	29.2
HCT116	colon	KCHA10[32]	21.3
LH86	liver	TLS11a[33] [c]	7.0
HBE135-E6E7[d]	lung	N/A	N/A

[a] sgc8c is a truncated DNA of sgc8. [b] T2-KK1B10 is a truncated DNA of KK1B10. [c] TLS11a was originally developed for liver cancer. [d] Normal cell line.

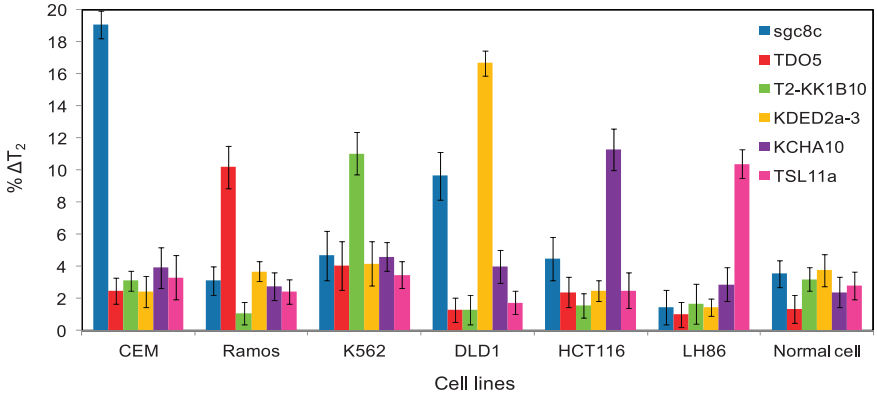

Figure 5. Use of magnetic nanosensors for pattern recognition of cancer cells. The $\%\ \Delta T_2$ was obtained by incubating different ACMNPs with various target cancer cell lines or control normal cell lines. All the measurements were performed using 1000 cells in a 250 μL sample volume.

cell type. Compared to other techniques, for example, flow cytometry (requiring $\sim 10^5$ cells)[34] and Western blot analysis (requiring $\sim 10^7$ cells),[34] the change of relaxation times from the MRSw technique shows good agreement with conventional methods by requiring fewer cells. Without any complexity of instrumental setting, MRSw also offers the advantages of simplicity, minimal detection time, and robustness under different sample conditions but still provides low detection limits. With such capabilities, the combination of ACMNPs and the MRSw technique could be further used for point-of-care detection, especially the analysis of clinical specimens, which normally contain both diseased and normal cells. Furthermore, the ability to profile cancer cells could be potentially utilized to monitor metastases or malignancy progression.

CONCLUSIONS

In summary, we have developed a rapid and sensitive nanosensor for the detection of cancer cells, as well as a method of profiling cancer cells based on MRSw. The ACMNPs were found to maintain their biological recognition and provide a multivalent effect, resulting in strong interaction with their target cells. Significantly, high sensitivity and specificity could be achieved by this nanosensor for the sample assays in complex biological systems, including serum, plasma, and whole blood. An array of ACMNPs was utilized to generate a distinct pattern recognition for multiple types of cancer cells. The nanosensor allowed not only the identification of cancer cells but also the differentiation between cancerous and normal cells. Notably, the reported technique does not require the use of complicated instruments, needing only a magnetic relaxation instrument with easy operation, making it widely accessible. In summary, the ACMNPs-based nanosensor holds great promise as a useful tool for reliable and sensitive detection, as well as cancer screening for clinical use.

MATERIALS AND METHODS

Synthesis of DNA Aptamers. The aptamers with strong affinities toward their intact tumor cells were selected by cell-SELEX and were chosen as demonstrated in Table 1. All aptamers were synthesized using standard phosphoramidite chemistry with an ABI3400 DNA/RNA synthesizer (Applied Biosystems, CA, USA). Biotin controlled pore glass from Glen Research was used for the synthesis. After the synthesis, the aptamers were deprotected in concentrated AMA (1:1 mixture of ammonium hydroxide and aqueous methylamine) solution at 65 °C for 30 min prior to further purification with reversed phase high-pressure liquid chromatography (RP-HPLC) on a ProStar HPLC Station (Varian, CA, USA) equipped with fluorescence and photodiode array detectors using a C-18 column (Econosil, C-18, 5 μM, 250 $\times$ 4.6 mm) from Alltech (Deerfield, IL, USA). The eluent was 100 mM triethylamine-acetic acid buffer (TEAA, pH 7.5) and acetonitrile (0−30 min, 10−100%). The collected DNA products were dried and detritylated with acetic acid. The detritylated aptamers were precipitated with ethanol and dried with a vacuum drier. The purified aptamers were then dissolved in DNA-grade water and quantified by determining the UV absorption at 260 nm using a UV−vis spectrometer (Cary 100, Varian, CA, USA).

Aptamer−Nanoparticle Conjugation. In order to prepare aptamer-conjugated magnetic nanoparticles, 30 nm streptavidin-coated iron oxide nanoparticles (Ocean Nanotech) were dispersed at 0.1 mg/mL in 100 mM PBS, pH 7.4. An excess amount of biotin-labeled aptamer was then added to the streptavidin-coated MNP solution. The mixture was vortexed at room temperature for 1 h, followed by three washings with PBS buffer using centrifugation at 14 000 rpm to remove any aptamers that did not conjugate to the MNPs. Zeta potential measurements were performed using a Brookhaven ZetaPlus at 25 °C to determine the successful conjugation of aptamers on MNP surface. The ACMNPs were dispersed in PBS and stored at 4 °C at a concentration of 0.1 mg/mL.

Cells and Culture Conditions. The cell lines listed in Table 1 were obtained from the American Type Culture Collection (ATCC). CCRF-CEM, Ramos, and DLD1 cells were cultured in RPMI 1640 medium (ATCC). K562 cells were maintained in culture with IMDM (ATCC). HCT116 cells were grown with McCoy's 5A (ATCC), and LH86 cells were maintained in culture with DMEM (ATCC). All media for cancer cells were supplemented with 10% heat-inactivated FBS and 100 U/mL penicillin−streptomycin. HBE135-E6E7, normal bronchial lung cell line, was maintained in keratin serum free medium supplemented with 5 ng/mL human recombinant epidermal growth factor , 0.05 mg/mL bovine pituitary extract (Invitrogen), 0.005 mg/mL insulin, and 500 ng/mL hydrocortisone. All cultured cells were grown in a humidified incubator at 37 °C under a 5% CO_2 atmosphere. In order to obtain single-cell suspensions for the binding studies of adherent cells, cells were cultured overnight in low density and treated with nonenzymatic cell dissociation solution (MP Biomedicals) for 5 min. Cells were aspirated several times, and the single cells were pelleted and washed twice before use in the binding assays. Cell suspensions were centrifuged at 1000 rpm for 5 min, and the pellet was resuspended in 2 mL of washing buffer. Ten microliter aliquots of the cell suspension were mixed with 10 μL of trypan blue solution. Cell quantification was performed using a hemacytometer (Hausser Scientific) and a microscope (Olympus). After determining the cell concentration, serial dilution of cells was prepared in PBS, FBS, plasma, or whole blood and used immediately after preparation.

Determination of Conjugated Nanoparticle−Cell-Specific Targeting. To demonstrate specific targeting, CCRF-CEM cells with their corresponding aptamer and fluorescein amidite (FAM)-labeled sgc8c were used, and FAM-labeled TDO5 was selected as a negative control. The sgc8c-ACMNPs were incubated with approximately one million CCRF-CEM cells, with the final concentration of 30 μg Fe/mL at 4 °C for 20 min in PBS. Similarly, TDO5-ACMNPs were also incubated with CCRF-CEM cells as a negative control. After incubation, the cells were washed twice to remove unbound ACMNPs and resuspended in PBS. The binding of aptamer-conjugated nanoparticles with target cells was investigated using a laser scanning confocal microscope setup consisting of an Olympus IX-81 inverted microscope with an Olympus Fluoview 500 confocal scanning system and a HeNe laser with a photomultiplier tube for detection. The cellular images were taken with a 20$\times$ objective. The ACMNPs were excited at 488 nm (λ_{ex} for FAM), and the emission was detected with a 505−525 nm band-pass filter.

Sample Assays Using Spin−Spin Relaxation Time Measurement. To determine the specificity and sensitivity of the detection, 50 μL aliquots of CCRF-CEM cell suspensions with different numbers of cells (1 to 10^6 cells) were incubated with 200 μL of sgc8c-ACMNPs solution in PBS ([Fe] = 10 μg/mL) at 4 °C for 40 min at a final volume of 250 μL. Similarly, as a negative control, TDO5-ACMNPs were also incubated with the cells. The spin−spin relaxation times (T_2) were measured at 1.5 T by an mq60 NMR

analyzer (Minispec, Bruker, Germany) operating at 37 °C without a washing step. In order to mimic real clinical samples, which normally contain thousands of different species, similar experiments were also performed in FBS, plasma, and whole blood from Innovative Research. To generate the profiling of cancer cells, all cell types listed in Table 1 were dispersed in PBS, such that each sample would contain only one cell type and approximately 1000 cells. Each type of ACMNP was incubated with each cell sample individually using the same conditions mentioned above, followed by the spin−spin relaxation time measurement.

Conflict of Interest: The authors declare no competing financial interest.

Acknowledgment. This work is supported by grants awarded by the National Institutes of Health (GM066137, GM079359 and CA133086), by the National Key Scientific Program of China (2011CB911000) and China National Grand Program (2009ZX-10004-312) and by the National Natural Science Foundation of China (20975034).

Supporting Information Available: Dynamic range determination of TDO5-ACMNPs for the detection of Ramos cells in PBS, the use of sgc8c-ACMNPs for the detection of CCRF-CCRF-CEM cells in complex biological media, including human plasma and human blood, and detailed detection mechanism of the magnetic nanosensors. This material is available free of charge *via* the Internet at http://pubs.acs.org.

REFERENCES AND NOTES

1. Brody, E. N.; Gold, L. Aptamers as Therapeutic and Diagnostic Agents. *Rev. Mol. Biotechnol.* **2000**, *74*, 5–13.
2. Ellington, A. D.; Szostak, J. W. In Vitro Selection of RNA Molecules that Bind Specific Ligands. *Nature* **1990**, *346*, 818–822.
3. Tuerk, C.; Gold, L. Systematic Evolution of Ligands by Exponential Enrichment: RNA Ligands to Bacteriophage T4 DNA Polymerase. *Science* **1990**, *249*, 505–510.
4. Osborne, S. E.; Matsumura, I.; Ellington, A. D. Aptamers as Therapeutic and Diagnostic Reagents: Problems and Prospects. *Curr. Opin. Chem. Biol.* **1997**, *1*, 5–9.
5. Yang, C. J.; Jockusch, S.; Vicens, M.; Turro, N. J.; Tan, W. Light-Switching Excimer Probes for Rapid Protein Monitoring in Complex Biological Fluids. *Proc. Natl. Acad. Sci. U. S. A.* **2005**, *102*, 17278–17283.
6. Nutiu, R.; Li, Y. In Vitro Selection of Structure-Switching Signaling Aptamers. *Angew. Chem., Int. Ed.* **2005**, *44*, 1061–1065.
7. Herr, J. K.; Smith, J. E.; Medley, C. D.; Shangguan, D.; Tan, W. Aptamer-Conjugated Nanoparticles for Selective Collection and Detection of Cancer Cells. *Anal. Chem.* **2006**, *78*, 2918–2924.
8. Smith, J. E.; Medley, C. D.; Tang, Z.; Shangguan, D.; Lofton, C.; Tan, W. Aptamer-Conjugated Nanoparticles for the Collection and Detection of Multiple Cancer Cells. *Anal. Chem.* **2007**, *79*, 3075–3082.
9. Koh, I.; Josephson, L. Magnetic Nanoparticle Sensors. *Sensors* **2009**, *9*, 8130–8145.
10. Gossuin, Y.; Gillis, P.; Hocq, A.; Vuong, Q. L.; Roch, A. Magnetic Resonance Relaxation Properties of Superparamagnetic Particles. *Wiley Interdisciplinary Reviews: Nanomed. Nanobiotechnol.* **2009**, *1*, 299–310.
11. Haun, J. B.; Yoon, T.-J.; Lee, H.; Weissleder, R. Magnetic Nanoparticle Biosensors. *Wiley Interdiscip. Rev.: Nanomed. Nanobiotechnol.* **2010**, *2*, 291–304.
12. Weissleder, R.; Moore, A.; Mahmood, U.; Bhorade, R.; Benveniste, H.; Chiocca, E. A.; Basilion, J. P. In Vivo Magnetic Resonance Imaging of Transgene Expression. *Nat. Med.* **2000**, *6*, 351–354.
13. Zhao, M.; Beauregard, D. A.; Loizou, L.; Davletov, B.; Brindle, K. M. Non-Invasive Detection of Apoptosis using Magnetic Resonance Imaging and a Targeted Contrast Agent. *Nat. Med.* **2001**, *7*, 1241–1244.
14. Liu, W.; Dahnke, H.; Jordan, E. K.; Schaeffter, T.; Frank, J. A. In Vivo MRI using Positive-Contrast Techniques in Detection of Cells Labeled with Superparamagnetic Iron Oxide Nanoparticles. *NMR Biomed.* **2008**, *21*, 242–250.
15. Perez, J. M.; Josephson, L.; O'Loughlin, T.; Hogemann, D.; Weissleder, R. Magnetic Relaxation Switches Capable of Sensing Molecular Interactions. *Nat. Biotechnol.* **2002**, *20*, 816–820.
16. Yigit, M. V.; Mazumdar, D.; Lu, Y. MRI Detection of Thrombin with Aptamer Functionalized Superparamagnetic Iron Oxide Nanoparticles. *Bioconjugate Chem.* **2008**, *19*, 412–417.
17. Kaittanis, C.; Naser, S. A.; Perez, J. M. One-Step, Nanoparticle-Mediated Bacterial Detection with Magnetic Relaxation. *Nano Lett.* **2006**, *7*, 380–383.
18. Perez, J. M.; Simeone, F. J.; Saeki, Y.; Josephson, L.; Weissleder, R. Viral-Induced Self-Assembly of Magnetic Nanoparticles Allows the Detection of Viral Particles in Biological Media. *J. Am. Chem. Soc.* **2003**, *125*, 10192–10193.
19. Kaittanis, C.; Santra, S.; Perez, J. M. Role of Nanoparticle Valency in the Nondestructive Magnetic-Relaxation-Mediated Detection and Magnetic Isolation of Cells in Complex Media. *J. Am. Chem. Soc.* **2009**, *131*, 12780–12791.
20. Fang, X.; Tan, W. Aptamers Generated from Cell-SELEX for Molecular Medicine: A Chemical Biology Approach. *Acc. Chem. Res.* **2009**, *43*, 48–57.
21. Chen, Y.; Munteanu, A. C.; Huang, Y.-F.; Phillips, J.; Zhu, Z.; Mavros, M.; Tan, W. Mapping Receptor Density on Live Cells by Using Fluorescence Correlation Spectroscopy. *Chem.—Eur. J.* **2009**, *15*, 5327–5336.
22. Koh, I.; Hong, R; Weissleder, R; Josephson, L. Nanoparticle-Target Interactions Parallel Antibody-Protein Interactions. *Anal. Chem.* **2009**, *81*, 3618–3622.
23. Shangguan, D.; Li, Y.; Tang, Z.; Cao, Z. C.; Chen, H. W.; Mallikaratchy, P.; Sefah, K.; Yang, C. J.; Tan, W. Aptamers Evolved from Live Cells as Effective Molecular Probes for Cancer Study. *Proc. Natl. Acad. Sci. U. S. A.* **2006**, *103*, 11838–11843.
24. Shangguan, D.; Cao, Z.; Meng, L.; Mallikaratchy, P.; Sefah, K.; Wang, H.; Li, Y.; Tan, W. Cell-Specific Aptamer Probes for Membrane Protein Elucidation in Cancer Cells. *J. Proteome Res.* **2008**, *7*, 2133–2139.
25. Tang, Z.; Shangguan, D.; Wang, K.; Shi, H.; Sefah, K.; Mallikratchy, P.; Chen, H. W.; Li, Y.; Tan, W. Selection of Aptamers for Molecular Recognition and Characterization of Cancer Cells. *Anal. Chem.* **2007**, *79*, 4900–4907.
26. Mallikaratchy, P.; Tang, Z.; Kwame, S.; Meng, L.; Shangguan, D.; Tan, W. Aptamer Directly Evolved from Live Cells Recognizes Membrane Bound Immunoglobin Heavy Mu Chain in Burkitt's Lymphoma Cells. *Mol. Cell. Proteomics* **2007**, *6*, 2230–2238.
27. Deng, T.; Li, J.; Zhang, L.-L.; Jiang, J.-H.; Chen, J.-N.; Shen, G.-L.; Yu, R.-Q. A Sensitive Fluorescence Anisotropy Method for the Direct Detection of Cancer Cells in Whole Blood Based on Aptamer-Conjugated Near-Infrared Fluorescent Nanoparticles. *Biosens. Bioelectron.* **2011**, *25*, 1587–1591.
28. Medley, C. D.; Smith, J. E.; Tang, Z.; Wu, Y.; Bamrungsap, S.; Tan, W. Gold Nanoparticle-Based Colorimetric Assay for the Direct Detection of Cancerous Cells. *Anal. Chem.* **2008**, *80*, 1067–1072.
29. Lee, H.; Sun, E.; Ham, D.; Weissleder, R. Chip-NMR Biosensor for Detection and Molecular Analysis of Cells. *Nat. Med.* **2008**, *14*, 869–874.
30. Chen, Y.; O'Donoghue, M. B.; Huang, Y.-F.; Kang, H.; Phillips, J. A.; Chen, X.; Estevez, M. C.; Yang, C. J.; Tan, W. A Surface Energy Transfer Nanoruler for Measuring Binding Site Distances on Live Cell Surfaces. *J. Am. Chem. Soc.* **2010**, *132*, 16559–16570.
31. Sefah, K.; Tang, Z. W.; Shangguan, D. H.; Chen, H.; Lopez-Colon, D.; Li, Y.; Parekh, P.; Martin, J.; Meng, L.; Phillips, J. A.; Kim, Y. M.; Tan, W. H. Molecular Recognition of Acute Myeloid Leukemia using Aptamers. *Leukemia* **2009**, *23*, 235–244.
32. Sefah, K.; Meng, L.; Lopez-Colon, D.; Jimenez, E.; Liu, C.; Tan, W. DNA Aptamers as Molecular Probes for Colorectal Cancer Study. *PLoS One 5*, e14269.
33. Shangguan, D.; Meng, L.; Cao, Z. C.; Xiao, Z.; Fang, X.; Li, Y.; Cardona, D.; Witek, R. P.; Liu, C.; Tan, W. Identification of

Liver Cancer-Specific Aptamers Using Whole Live Cells. *Anal. Chem.* **2008**, *80*, 721–728.
34. Lee, H.; Yoon, T.; Figueiredo, J.; Swirski, F. K.; Weissleder, R. Rapid Detection and Profiling of Cancer Cell in Fine-Needle Aspirates. *Proc. Natl. Acad. Sci. U. S. A.* **2009**, *106*, 12459–12464.
35. El-Boubbou, K.; Zhu, D. C.; Vasileiou, C.; Borhan, B.; Prosperi, D.; Li, W.; Huang, X. Magnetic Glyco-Nanoparticles: A Tool To Detect, Differentiate, and Unlock the Glyco-Codes of Cancer via Magnetic Resonance Imaging. *J. Am. Chem. Soc.* **2010**, *132*, 4990–4999.